ACS APPLIED MATERIALS & INTERFACES

Letter

www.acsami.org

Influence of Seeding and Bath Conditions in Hydrothermal Growth of Very Thin (~20 nm) Single-Crystalline Rutile TiO_2 Nanorod Films

Seare A. Berhe,[†] Soumya Nag,[‡] Zachary Molinets,[†,§] and W. Justin Youngblood*[,†]

[†]Department of Chemistry and [‡]Department of Materials Science and Engineering and Center for Advanced Technology, University of North Texas, Denton, Texas 76203, United States

Supporting Information

ABSTRACT: New seeding conditions have been examined for the hydrothermal growth of single-crystalline rutile TiO_2 nanorods. Rutile nanorods of ~20 nm diameter are grown from seed layers consisting of either (A) TiO_2 or MnOOH nanocrystals deposited from suspension, or (B) a continuous sheet of TiO_2. These seed layers are more effective for seeding the growth of rutile nanorods compared to the use of bare F-SnO_2 substrates. The TiO_2 sheet seeding allows lower concentration of titanium alkoxide precursor relative to previously reported procedures, but fusion of the resulting TiO_2 nanorods into bundles occurs at higher precursor concentration and/or longer growth duration. Performance of polymer-oxide solar cells prepared using these nanorods shows a dependence on the extent of bundling as well as rod height.

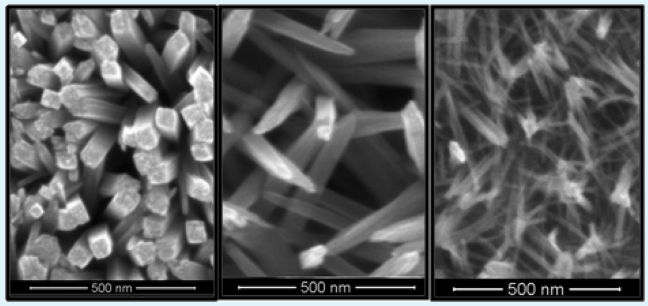

KEYWORDS: *single-crystalline, rutile, TiO_2, hydrothermal, growth, control, morphology, polymer, oxide, solar, cell*

Nanostructured films of oxide semiconductors such as titanium dioxide (TiO_2) with one-dimensional morphology are useful for solid-state dye solar cells, polymer-oxide solar cells, photoelectrochemical solar cells, and photocatalytic materials.[1−6] Nanorod films are easier to infiltrate with semiconductive polymers, molecular hole conductors, and supramolecular or nanoparticulate species compared to films of nanoparticle-based mesoporous oxide semiconductors.[7−10] Additionally, electron transport in a given oxide semiconductor is faster in one-dimensional assemblies than in to nanoparticle-based films.[11−13] Films of single-crystalline nanorods with only one crystal face exposed may be useful for transient spectroscopy of sensitized oxide semiconductors,[14] because they have less diversity of interfaces compared to nanoparticle-based films and have higher surface area than bulk single-crystals. The surface area for nanorod-based films is lower than for nanoparticle-based films of equivalent height, so photocurrents produced from films of sensitized oxide nanorods are generally lower than for mesoporous oxide films. To enhance the surface area of single-crystalline rutile TiO_2 nanorod films, nanorods of narrow diameter (<50 nm) and dense packing are needed.

Several methods for the hydrothermal growth of single-crystalline rutile TiO_2 nanorods have now been reported.[13,15−20] Their general principle is the use of superheated water or a mixture of superheated water with an organic cosolvent to achieve solution conditions that favor the deposition of TiO_2 from solvated Ti(IV) species. Superheated water exhibits a reduced dielectric constant,[21] greater self-dissociation into hydronium and hydroxide,[22] and greater miscibility with organic solvents.[23] Preferential growth along the [001] crystal axis is observed because of inhibition of growth at the [110] axis by coordination of Cl ions in the growth bath.[16,17,24,25] Grimes and co-workers first reported the hydrothermal/solvothermal synthesis of rutile TiO_2 nanorods of 10−35 nm diameter from a toluene/HCl (10 M) mixture using a sol−gel-derived TiO_2 seed layer on F-SnO_2 (FTO).[15,18] This method uses an extremely high concentration of titanium precursors in the growth bath (270 mM $Ti(OiPr)_4$ + 700 mM $TiCl_4$) and presents difficulty in reproducibly preparing thin films (<1 μm) because the initial growth is rapid. Mullins and co-workers have reported using n-hexane as the organic phase with lower concentration of [Ti] (150−300 mM) to produce thin nanorods (5 nm diameter), although considerable fusion of their nanorod films occurred upon annealing.[16] Mallouk and co-workers have found that using butanone as the organic phase and yet lower [Ti] (100−200 mM $Ti(OBu)_4$) gave nanorods of 40 nm diameter.[13] Liu and Aydil grew rutile TiO_2 nanorods directly on FTO substrates from 5 M HCl (aq) without any seed layer or organic solvent.[17] An added benefit of the Liu/Aydil procedure is the further-reduced [Ti] (55 mM $Ti(OiPr)_4$) relative to the Grimes/Mullins/Mallouk methods, although the Liu/Aydil nanorods are generally thicker (100 nm diameter). Although Liu and Aydil observed that the TiO_2 nanorods did not grow on unseeded surfaces of Si or SiO_2, Zhou and co-workers reported the growth of rutile TiO_2

Received: October 12, 2012
Accepted: February 6, 2013
Published: February 6, 2013

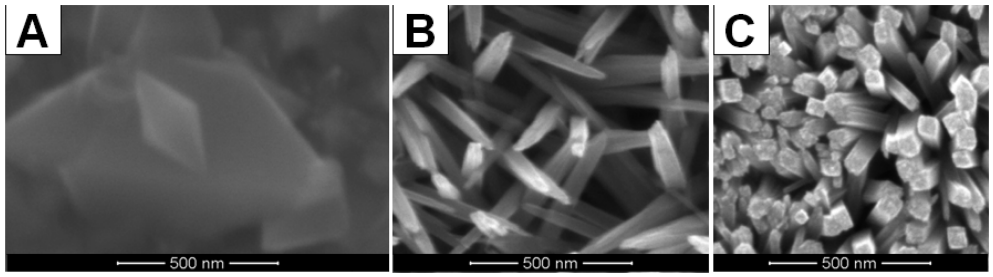

Figure 1. Rutile TiO_2 grown using the method from ref 17 on (A) bare 7 Ohm/square FTO, (B) a seed layer of MnOOH nanoparticles on FTO, or (C) a continuous sheet of TiO_2 on FTO. Growth time was 4 h for film A, and 2 h for each of films B and C. Film A is too rough for an average film height, but films B and C were measured at 800 and 750 nm (±50 nm), respectively.

nanorods and "dandelion" multilayers of nanorods on arbitrary substrates, simply by elevating the [Ti] in the aqueous growth bath to 165 mM.[18] Wang and co-workers reported growth on arbitrary substrates using a seed layer of sol−gel TiO_2, obtaining nanorods of ∼100 nm diameter despite lowering the [Ti] to 33 mM.[19] Finally, Dong and co-workers showed TiO_2 nanorod growth from untreated titanium surfaces.[20] We report herein methods using transparent seed layers that remove the reliance on FTO as a seeding substrate using low [Ti] (28 mM) and achieve monolayer films of thin nanorods (∼20 nm).

In reproducing the Liu/Aydil procedure, we found that the method is sensitive to the type of FTO. Using FTO with 7 Ohm/square resistivity instead of the 15 Ohm/square FTO reported in the earlier method, we obtained large crystal grains of rutile TiO_2 (Figure 1A) but no nanorods. Given the evidence that rutile SnO_2 in the FTO acts as a seed layer for the direct growth of rutile TiO_2,[17] we attribute this outcome to a difference in the surface roughness in lower resistivity FTO. Commercial FTO substrates achieve lower resistivity through the layer thickness of the FTO, and thicker films of FTO need lower surface roughness to minimize haze.[26] In a search for alternative seeding methods, we have discovered that thin single-crystalline (20 nm) rutile TiO_2 nanorods can be grown using a seed layer of manganese oxyhydroxide (MnOOH) nanoparticles (Figure 1B) or a seed layer of TiO_2 comprised of either a thin conformal sheet of TiO_2 (Figure 1C) or a film of rutile TiO_2 nanoparticles (see Figure S18 in the Supporting Information). The single-crystallinity of the nanorods was confirmed by small-area electron diffraction (SAED-TEM; see Figures S1 and S2 in the Supporting Information). The nanorods are prone to fuse into small or large bundles depending on the seeding and bath conditions used for their growth.

Rutile TiO_2 nanoparticles can be spin-coated onto substrates from aqueous suspension and annealed into a stable seeding layer. Although dense nanorod films can be grown from such seeding (see Figure S18 in the Supporting Information), almost all films prepared from using rutile TiO_2 seeding exhibited peeling from the substrate and/or severe cracking. MnOOH nanoparticles, produced by reduction of $KMnO_4$ with a primary alcohol, were first reported as a seed layer for the growth of ZnO nanorods by Hodes and co-workers.[27] Whether the nanoparticles are actually MnOOH or MnO_2 is not definitively known. Rutile TiO_2 nanowires grown from these seeds appear to form in small bundles of just a few nanorods, and at varying angles relative to the surface normal (Figure 1B). Films can be grown as short as 200 nm or as tall as 8 μm, but low growth angles inhibit the growth of many of the nanorods in taller films.

A thin layer of thermally evaporated titanium metal (10−20 nm) can be annealed to 450 °C under ambient atmosphere to obtain a continuous transparent seed layer of TiO_2. Hydrothermal growth from this thin TiO_2 underlayer using the conditions of Liu and Aydil produces a dense film of TiO_2 nanorods (Figure 1C) that we initially estimated at ∼100 nm diameter.[28] Closer inspection of our films have led us to realize that the ∼100 nm diameter 'rods' were actually bundles of much smaller (∼20 nm) nanorods. Fusion of the nanorods is a consequence of the [110] crystal face being the only surface at all sides of the nanorods. Mullins and co-workers reported that such bundling was dependent on the choice of titanium precursor and organic cosolvent, and their films of TiO_2 nanorods were either unbundled or severely bundled. In our observation, the bundling shows dependence on the seeding method, the concentration of the titanium precursor, and the growth height of the film. Films of just 200 nm thickness grown at 55 mM [Ti] show individual nanorods of 40 nm diameter (Figure 2). At film heights above 1 μm, bundling becomes so severe that the films are nearly continuous (see Figure S17 in the Supporting Information). Reducing the concentration of the titanium alkoxide precursor from 55 to 28 mM provides a less dense seeding, which in turn reduces the extent of nanorod bundling (Figure 3). In a 200 nm tall film (Figure 3A) grown at 28 mM [Ti], there are individual nanorods of 20 nm diameter as well as locations where nanorods are coming together to form bundles. In 6 h of growth, films of ∼2 μm (Figure 3B) are formed with some bundles enclosing a few or several nanorods. Film growth for durations longer than 6 h provided diminishing returns on nanorod height, but a given film can be resubmitted to a fresh bath solution for further growth. Unfortunately, the surface area gained by additional height is more than offset by surface area loss due to rod fusion. A film grown to 5 μm height

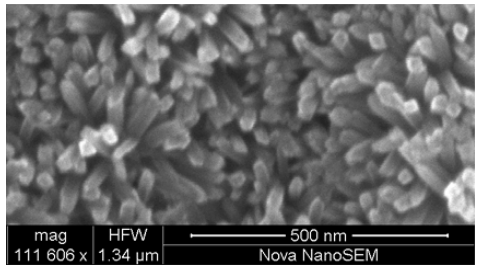

Figure 2. Rutile TiO_2 nanorods grown to just 200 nm height with minimal bundling of the nanorods.

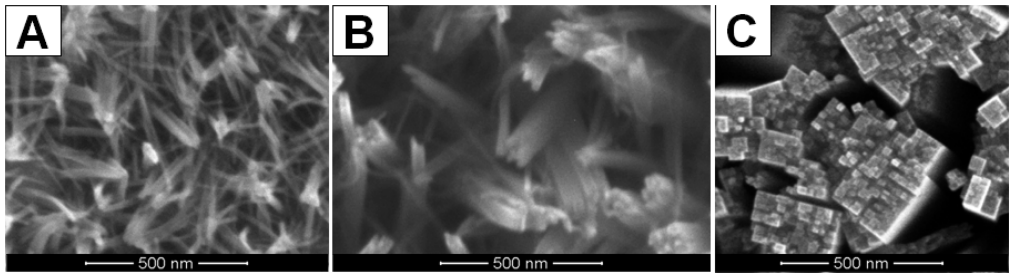

Figure 3. Films of rutile TiO_2 nanorods grown to heights of (A) 200 nm, (B) 2 μm, and (C) 5 μm under identical growth conditions.

by two consecutive 6 h growths has severe fusion (Figure 3C). Only the TiO_2 sheet layer showed growth at 28 mM [Ti], and at concentrations of the $Ti(iOPr)_4$ below 28 mM, we did not observe nanorod growth. Additional SEM images of TiO_2 nanorod films grown to different heights with all seeding methods at varying [Ti] can be found in the Supporting Information.

The parameters that differentiate these seeding methods from each other as well as from previously reported methods or the use of bare FTO are the size and spacing of seeding domains. When the nanorod seeding is dense, rods with low growth angles terminate quickly and serve as new seeding points, with the overall effect of producing densely packed epitaxially oriented nanorods that are prone to bundling. The thin conformal coating of TiO_2 on FTO cannot be distinguished from bare FTO by SEM imaging (Figure 4, A vs B). Because TiO_2 should be a better seeding surface than FTO for the growth of TiO_2, the conformal TiO_2 coating should lead to the growth of rutile crystals for TiO_2/FTO substrates that are at least as large as observed for bare FTO, but instead we observed nanorod growth. Lira-Cantu and co-workers have shown that thin sheets of TiO_2 on FTO have both anatase and rutile domains,[29] and more favorable seeding at the rutile domains within a mixed-phase seed layer may explain the small size of nanorods grown in the film. Additionally, the initial treatment of the TiO_2/FTO substrates in 5 M HCl prior to reaching growth temperature (150 °C) may cause some etching of the TiO_2 surface that could contribute to the small seeding domains, as reported for growth on titanium substrates.[20] Growth at 28 mM [Ti] results in a lower density of nanorods,[17] so bundling is less severe at lower growth heights, but progresses as the film is grown taller. For np-MnOOH seed layers (Figure 4C), Hodes and co-workers reported the deposition of well-dispersed nanoparticles that are each just a few nanometers in diameter. In our case, although such small particles may be present, we could not resolve any image of them but we do see large textured aggregates of MnOOH nanoparticles that do not completely cover the FTO surface. The lower seeding density and amorphous texture of the np-MnOOH deposits results in nanorod growth at lower angles to the surface and less bundling compared to the TiO_2-sheet seeding. We observed no delamination of films grown from np-MnOOH seeding or films grown at 28 mM [Ti] from a TiO_2 sheet layer, with growth times as long as 18 h. The previously reported delamination of TiO_2 nanorod films[17] from the underlying FTO substrate occurs only with films having denser seeding/growth of nanorods, such as the films grown at 55 mM [Ti] from either TiO_2 sheet or a spin-coated film of rutile TiO_2 nanoparticles. Films grown from np-TiO_2 seeding delaminated if grown longer than 4 h, whereas films grown from a TiO_2 sheet at 55 mM [Ti] could be grown up to 7 h without delamination.

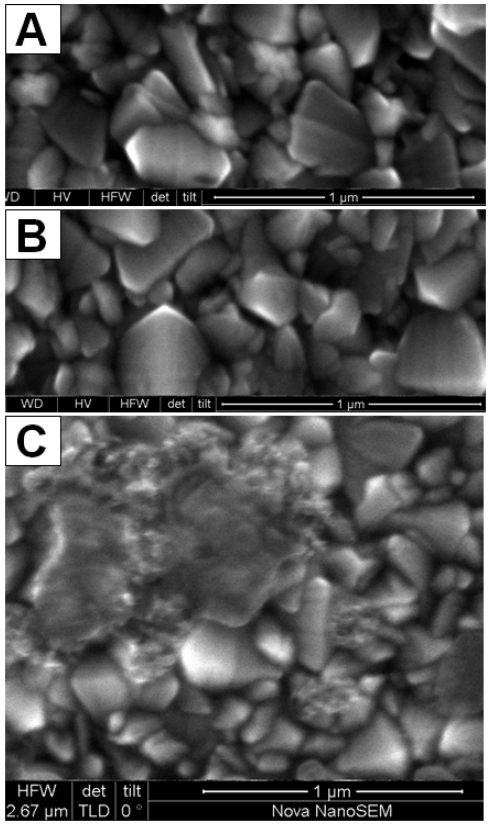

Figure 4. Substrates used for TiO_2 nanorod growth: (A) bare FTO, (B) a 10 nm-thick coating of TiO_2 on FTO, and (C) MnOOH nanoparticles on FTO.

One example of the issues that can be addressed using such easily prepared films is the variation of nanorod film thickness in hybrid inverted organic photovoltaic (HOPV) cells using a semiconductive polymer with TiO_2 nanorods. Bulk heterojunction organic photovoltaic cells such as those using P3HT and a methanofullerene (PCBM) are kept to 200−350 nm thickness to accommodate the slower mobility of charge carriers in the organic semiconductors relative to inorganic semiconductors, despite inadequate light absorption in such thin films. HOPV cells are generally kept to the same thickness, although it has been proposed that the confinement of an organic semiconductor into a low-dimensional morphology should allow for operation of devices with thicker active layers.[30] Additionally, polymer oxide cells have one domain, the oxide semiconductor, with faster carrier transport. Rutile TiO_2, for example, has an electron mobility of ~1 $cm^2/(V\ s)$.[31] We explored the influence of film thickness on the performance of

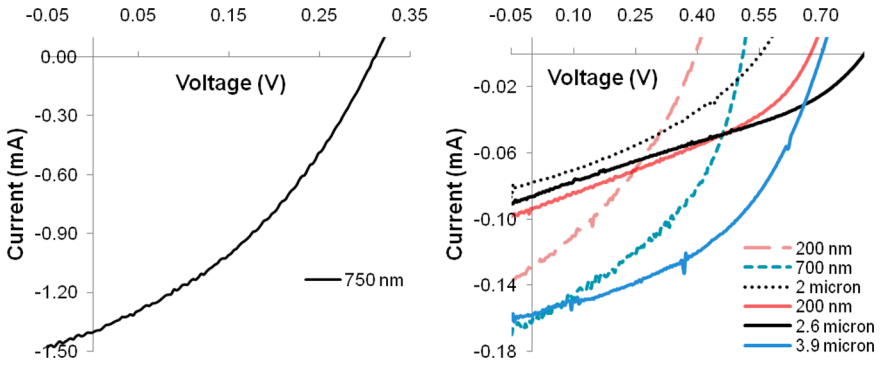

Figure 5. Current−voltage behavior of photovoltaic cells using the grown TiO_2 nanorod films. All devices were prepared from films seeded with a continuous TiO_2 sheet seed layer. Legends indicate height of the nanorods films used. Solid line traces indicate films grown at 55 mM [Ti], whereas dotted/dashed traces indicate films grown at 28 mM [Ti].

polymer-oxide solar cells composed of poly(3-hexylthiophene) (P3HT) and rutile TiO_2 nanorod films grown to heights of 200−3900 nm from baths of either 55 or 28 mM [Ti]. Photovoltaic test devices with active areas of 1 cm^2 were assembled on FTO electrodes with rutile TiO_2 nanorod films. Details of the device assembly methods are provided in the Supporting Information.

Figure 5 shows the current−voltage behavior of the prepared devices. Films grown at 55 mM $Ti(iOPr)_4$ to a height of 750 nm (Figure 1C) gave significantly higher photocurrent and lower photovoltage than all other films. The stark difference in behavior is most logically explained by the difference in the proportion of the active layer that is at the polymer/oxide interface versus away from the interface (i.e., in the 'bulk'), with greater proportion of material at the interface leading to more charge separation, and thus more photocurrent, but also more charge recombination, and therefore lower photovoltage. The bundling of nanorods results in narrower void channels between TiO_2 nanorods. Where gaps between nanorods are thin (<20 nm), excitons generated in the polymer can reach the polymer/oxide interface before decaying, and free carriers generated within the polymer can reach the oxide surface before recombining. One pathway to better nanorod spacing could be the use of substrates with greatly reduced surface roughness.

In conclusion, we have discovered new seeding methods for the growth of single-crystalline rutile TiO_2 nanorod films and shown the dependence of rod fusion upon seeding density. In particular, we report a facile method for producing films of thin (20 nm) rutile nanorods up to 2 μm in height without severe bundling. This method consumes less titanium reagent than any other method so far reported for the growth of such films. The low photocurrents of the solar cells examined in this study are an indication that further optimization of the nanorod morphology is needed. These easily grown TiO_2 nanorod films will be especially useful to researchers working with polymers, macromolecules, or chemically synthesized nanoparticles that cannot easily be loaded into nanoparticulate TiO_2 films.

■ ASSOCIATED CONTENT

Supporting Information

TEM and SAED characterization of the TiO_2 nanorods, charts of film growth rates, profilometry data and additional SEM images of nanorods films, dark current−voltage behavior of photovoltaic devices, and UV−vis absorption data of dye-sensitized nanorods films. This information is available free of charge via the Internet at http://pubs.acs.org.

■ AUTHOR INFORMATION

Corresponding Author

*E-mail: youngblood@unt.edu.

Present Address

[§]Department of Chemistry, Purdue University, West Lafayette, Indiana 47907, United States

Notes

The authors declare no competing financial interest.

■ ACKNOWLEDGMENTS

We thank the UNT Center for Advanced Research and Technology (CART) for an instrument usage grant to conduct SEM and profilometry studies, the University of North Texas for startup funding and internal grants (FRG #s GA9550 and GA9154), and the UNT McNair Scholars Program for a scholarship supporting Z. Molinets.

■ REFERENCES

(1) Wang, M.; Bai, J.; Le Formal, F.; Moon, S.-J.; Cevey-Ha, L.; Humphry-Baker, R.; Gratzel, C.; Zakeeruddin, S. M.; Gratzel, M. *J. Phys. Chem. C* **2012**, *116*, 3266−3273.
(2) Shankar, K.; Mor, G. K.; Prakasam, H. E.; Varghese, O. K.; Grimes, C. A. *Langmuir* **2007**, *23*, 12445−12449.
(3) Toyoda, T.; Shen, Q. *J. Phys. Chem. Lett.* **2012**, *3*, 1885−1893.
(4) Kamat, P. V. *J. Phys. Chem. C* **2007**, *111*, 2834−2860.
(5) Chen, X.; Mao, S. S. *Chem. Rev.* **2007**, *107*, 2891−2959.
(6) Hwang, Y. J.; Hahn, C.; Liu, B.; Yang, P. *ACS Nano* **2012**, *6*, 5060−5069.
(7) Boucle, J.; Ravirajan, P.; Nelson, J. *J. Mater. Chem.* **2007**, *17*, 3141−3153.
(8) Borchert, H. *Energy Environ. Sci* **2010**, *3*, 1682−1694.
(9) Baeten, L.; Conings, B.; Boyen, H.-G.; D'Haen, J.; Hardy, A.; D'Olieslaeger, M.; Manca, J. V.; Van Bael, M. K. *Adv. Mater.* **2011**, *23*, 2802−2805.
(10) Coakley, K. M.; Liu, Y.; McGehee, M. D.; Frindell, K. L.; Stucky, G. D. *Adv. Funct. Mater.* **2003**, *13*, 301−306.
(11) Kamat, P. V.; Tvrdy, K.; Baker, D. R.; Radich, J. G. *Chem. Rev.* **2010**, *110*, 6664−6688.
(12) Hochbaum, A. I.; Yang, P. *Chem. Rev.* **2010**, *110*, 527−546.
(13) Feng, X.; Zhu, K.; Frank, A. J.; Grimes, C. A.; Mallouk, T. E. *Angew. Chem.* **2012**, *124*, 2781−2784.
(14) Spitler, M. T.; Parkinson, B. A. *Acc. Chem. Res.* **2009**, *42*, 2017−2029.
(15) Feng, X.; Shankar, K.; Varghese, O. K.; Paulose, M.; Latempa, T. J.; Grimes, C. A. *Nano Lett.* **2008**, *8*, 3781−3786.

(16) Hoang, S.; Guo, S.; Hahn, N. T.; Bard, A. J.; Mullins, C. B. *Nano Lett.* **2012**, *12*, 26−32.
(17) Liu, B.; Aydil, E. S. *J. Am. Chem. Soc.* **2009**, *131*, 3985−3990.
(18) Kumar, A.; Madaria, A. R.; Zhou, C. *J. Phys. Chem. C* **2010**, *114*, 7787−7792.
(19) Wang, H.-E.; Chen, Z.; Leung, Y. H.; Luan, C.; Liu, C.; Tang, Y.; Yan, C.; Zhang, W.; Zapien, J. A.; Bello, I.; Lee, S.-T. *Appl. Phys. Lett.* **2010**, *96*, 263104.
(20) Dong, L.; Cheng, K.; Weng, W.; Song, C.; Du, P.; Shen, G.; Han, G. *Thin Solid Films* **2011**, *519*, 4634−4640.
(21) Akerlof, G. C.; Oshry, H. I. *J. Am. Chem. Soc.* **1974**, *72*, 2844−2847.
(22) Marshall, W. L.; Franck, E. U. *J. Phys. Chem. Ref.* **1982**, *10*, 295−304.
(23) Siskin, M.; Katritzky, A. R. *Chem. Rev.* **2001**, *101*, 825−835.
(24) Pottier, A.; Chaneac, C.; Tronc, E.; Mazerolles, L.; Jolivet, J.-P. *J. Mater. Chem.* **2011**, *11*, 1116−1121.
(25) Allen, P. B. *Nano Lett.* **2007**, *7*, 6−10.
(26) Szanyi, J. *Appl. Surf. Sci.* **2002**, *185*, 161−171.
(27) Kokotov, M.; Hodes, G. *J. Mater. Chem.* **2009**, *19*, 3847−3854.
(28) Berhe, S. A.; Zhou, J. Y.; Haynes, K. M.; Rodriguez, M. T.; Youngblood, W. J. *ACS Appl. Mater. Interfaces* **2012**, *4*, 2955−2963.
(29) Lira-Cantu, M.; Chafiq, A.; Faissat, J.; Gonzales-Valls, I.; Yu, Y. *Sol. Energy. Mater. Sol. Cells* **2011**, *95*, 1362−1374.
(30) Coakley, K. M.; Srinivasan, B. S.; Ziebarth, J. M.; Goh, C.; Liu, Y.; McGehee, M. D. *Adv. Funct. Mater.* **2005**, *15*, 1927−1932.
(31) Kavan, L.; Gratzel, M.; Gilbert, S. E.; Klemenz, C.; Scheel, H. J. *J. Am. Chem. Soc.* **1996**, *118*, 6716−6723.